16th World Conference on Earthquake, 16WCEE 2017
Santiago Chile, January 9th to 13th 2017
Paper N° 3624
Registration Code: S-G1461170892

SEISMIC DESIGN AND PERFORMANCE OF REINFORCED CONCRETE BRIDGE COLUMN – ENLARGED PILE SHAFT CONNECTIONS

J. Murcia-Delso [(1)], Y. Liu [(2)], P.B. Shing [(3)]

[(1)] Senior Researcher, Sustainable Construction Division, Tecnalia Research & Innovation, juan.murcia@tecnalia.com
[(2)] Graduate Student Researcher, Department of Structural Engineering, University of California, San Diego, yliu8@ucsd.edu
[(3)] Professor, Department of Structural Engineering, University of California, San Diego, pshing@ucsd.edu

Abstract

This paper presents results of an experimental and analytical investigation conducted at the University of California, San Diego to improve the seismic design of column-enlarged pile shaft connections. Four full-scale column-shaft assemblies were tested under quasi-static cyclic lateral loading to study the minimum embedment length required for column reinforcement extended into an enlarged pile shaft and the necessary transverse reinforcement in the bar anchorage zone of a shaft to develop the necessary anchorage capacity and minimize splitting cracks. The test specimens had different column longitudinal bar sizes, different embedment lengths of the column reinforcement inside the shafts, and different amount of transverse reinforcement in the shafts. Experimental results have been complemented by nonlinear finite element analysis performed with an analytical bond-slip model developed and implemented in Abaqus to obtain a good understanding of the cyclic bond deterioration in the longitudinal reinforcement and to determine the minimum embedment length required. Based on the experimental and analytical results, new design recommendations have been developed. These recommendations can result in a significant reduction of the embedment length as compared to current seismic design specifications of the California Department of Transportation and AASHTO.

Keywords: bridge column, pile shaft, development length, large-scale testing, nonlinear finite element analysis

1. Introduction

Pile shafts are used frequently as foundations of reinforced concrete bridge columns because of the convenience in construction. When a pile shaft has the same diameter as the column it supports, plastic deformation is expected to form in the shaft below ground when the column is subjected to a severe seismic load. A pile shaft with a section larger than that of the column it supports is more convenient for post-earthquake inspection and repair because the plastic hinge will develop at the column base. However, because the column and shaft diameters are different, it is not possible to have a continuous reinforcing cage for both elements, and the column longitudinal reinforcement has to be extended into the shaft and form a non-contact lap splice with the longitudinal shaft reinforcement, as shown in Fig. 1.

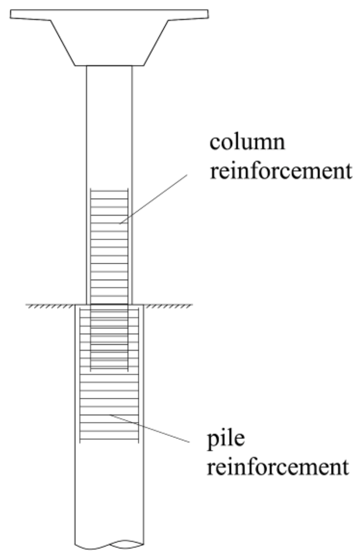

Fig. 1 – Bridge column supported on enlarged pile shaft

For reinforced concrete bridge columns supported on enlarged pile shafts, the Seismic Design Criteria of the California Department of Transportation [1] and the AASHTO LRFD Seismic Bridge Design Specifications [2] require that longitudinal bars in the columns be terminated in the pile shaft in a staggered manner with minimum embedment lengths of $D_{c,\max} + l_d$ and $D_{c,\max} + 2l_d$, respectively, where $D_{c,\max}$ is the larger cross-sectional dimension of the column, and l_d is the development length required for a straight bar in tension based on the expected material properties. In this specification, the required embedment length is governed by the column dimension $D_{c,\max}$ to account for a shortening of the effective development length caused by possible damage penetration into the embedment zone when plastic deformation develops at the column base. However, this requirement was determined to be very conservative based on the results of a study carried out by McLean and Smith [3].

This paper presents results of an investigation to develop new seismic design recommendations to minimize the development length of bridge column longitudinal bars in enlarged pile shafts. Four full-scale column-pile assemblies were tested under quasi-static cyclic lateral loading in the laboratory to study the conservatism of current specifications and validate new design formulas for the minimum embedment length of the column reinforcement and the amount of transverse reinforcement required in the bar anchorage region of a pile shaft. Nonlinear finite element analyses of the column-pile tests have been conducted to further the understanding of the bond-slip behavior and the development of column longitudinal reinforcement in oversized pile shafts.

2. Design formulas for column – enlarged pile shaft connections

2.1 Minimum embedment length of column reinforcement

Current Caltrans and AASHTO LRFD specifications can result in embedment lengths significantly longer than the tension development length specified in the AASHTO LRFD Bridge Design Specification [4] because of the additional length $D_{c,\max}$. The study by McLean and Smith [3] has shown that non-contact lap splices in oversized pile shafts can perform in a satisfactory manner with a lap splice length equal to $l_s + s$, where $l_s = 1.7 \times l_d$, which is the lap length specified for Class C splice in AASHTO [4], and s is the bar spacing in the non-contact lap splice. The length proposed by McLean and Smith [3] is based on a truss model that assumes that force transfer between the spliced bars is through 45-degree-angle compression struts. This length was validated with experimental data from reduced-scale tests on column-pile connections. The applicability of this recommendation to large-size columns and large-diameter bars had not been verified.

Based on data from development length tests of large-diameter bars embedded in concrete specimens with reinforcement details similar to those in an enlarged pile shaft and a numerical study using nonlinear finite element models, Murcia-Delso et al. [5] have suggested that the embedment length, l_e, can be further reduced to that given by Eq. (1).

$$l_e = l_d + s + c \tag{1}$$

in which c is the thickness of the concrete cover above the pile reinforcement and l_d is the tension development length specified in the AASHTO LRFD Bridge Design Specifications [4]. The term $s + c$ in this equation is to account for the ineffective force transfer region in the upper part of the non-contact lap splice as considered by McLean and Smith [3].

2.2 Transverse reinforcement in column anchorage region of the pile shaft

Transverse reinforcement is required in the embedment region of the column reinforcement inside the pile shaft to prevent a splitting failure of the anchorage. McLean and Smith [3] have proposed Eq. (2) to determine the maximum permissible spacing, $s_{tr,\max}$, of the transverse reinforcement to resist the strut force based on a truss analogy.

$$s_{tr,\max} = \frac{2\pi A_{tr} f_{y,tr} l_s}{A_l f_u} \tag{2}$$

in which A_l and f_u are the total cross-sectional area and tensile strength of the longitudinal reinforcement, A_{tr} and $f_{y,tr}$ are the cross-sectional area and yield strength of a transverse reinforcing bar, and $l_s = 1.7 \times l_d$.

Based on the study of the splitting forces inside the anchorage region of a pile shaft, Murcia-Delso et al. [5] have proposed Eq. (3) to determine the maximum permissible spacing of the transverse reinforcement in the bar anchorage region of a pile shaft.

$$s_{tr,\max} = \frac{2\pi A_{tr} f_{y,tr}}{N_{col} d_{b,col} \tau_{\max}} \tag{3}$$

in which N_{col} is the number of longitudinal bars in the column, $d_{b,col}$ is the diameter of the column longitudinal bars, and $\tau_{\max}$ is the maximum bond strength of the bars, which can be taken to be 16.5 MPa (2.4 ksi) for 34.5-MPa (5-ksi) concrete. For concrete strengths other than 34.5 MPa (5 ksi), $\tau_{\max}$ can be assumed to be proportional to $f_c'^{3/4}$, as suggested in Murcia-Delso et al. [6] for bars in well-confined concrete like that in a pile shaft. A more stringent requirement has also been proposed to control the width of tensile splitting cracks with an engineered steel casing. For the nominal width of the radial splitting cracks to be no greater than $u_{cr,\max}$, the minimum thickness, $t_{c,\min}$, of the steel casing should be:

$$t_{c,\min} = \frac{1}{\alpha_2 f_{y,c}} \left(\frac{1}{2\pi} N_{col} \tau_{\max} d_{b,col} - \alpha_1 \frac{A_{tr}}{s_{tr}} f_{y,tr} \right) \tag{4a}$$

in which $f_{y,c}$ is the nominal yield strength of the casing steel, s_{tr} is the spacing of the transverse hoops inside the pile, and α_1 and α_2 are calculated as follows.

$$\alpha_1 = \frac{u_{cr,\max} N_{sh}}{\pi D_{ext} \varepsilon_{y,tr}} \leq 1 \tag{4b}$$

$$\alpha_2 = \frac{u_{cr,\max} N_{sh}}{\pi D_s \varepsilon_{y,c}} \leq 1 \tag{4c}$$

in which N_{sh} is the number of pile longitudinal bars D_{ext} is the diameter of the pile transverse reinforcement, $\varepsilon_{y,tr}$ is the yield strain of the transverse reinforcement, D_s is the diameter of the steel casing, and $\varepsilon_{y,c}$ is the yield strain of the casing steel.

2 Large-scale testing of column-pile assemblies

2.1 Test specimens and setup

Four full-scale column-pile assemblies were tested under fully-reversed cyclic lateral loading. Each test specimen consisted of a bridge column and the upper portion of a pile shaft, as shown in Fig. 2. The geometry and reinforcing details of the specimens are shown in Table 1. The columns in these specimens had a diameter of 1219 mm (4 ft) and aspects ratios varying between 4 and 4.5. Specimens 1, 2, and 3 had 1829-mm (6-ft) diameter piles, and the fourth had a 1524-mm (5-ft) diameter pile. The size of the longitudinal reinforcing bars varied from No. 8 (25 mm) to No. 14 (43 mm) for the columns, and from No. 11 (36 mm) to No. 18 (57 mm) for the piles.

Specimen 1 was designed to represent existing bridge columns in California. The column reinforcement in Specimen 1 had an embedment length equal to $D_{c,\max} + l_d$. However, the requirement to terminate half of the longitudinal bars at $D_{c,\max} + 2l_d$ was not applied. This reduction was proved to be safe by a pre-test finite element analysis of the column-pile assembly. The transverse reinforcement in the entire pile segment was determined according to the design requirements for compression members in AASHTO [4].

In Specimens 2 through 4, the embedment length of the column reinforcement was reduced to $l_d + s + c$. For Specimen 2, the amount of transverse reinforcement in the bar anchorage region of the pile was determined based on the equation proposed by McLean and Smith [3]. Specimen 3 was identical to Specimen 2, except that the transverse reinforcement in the pile was reduced and a steel casing was added to the pile to ensure an adequate anchorage capacity and to control the width of the tensile splitting cracks. The thickness of the steel casing was determined with Eq. (4) and $u_{cr,\max}$ equal to 0.3 mm (0.012 in.), which is the maximum crack width recommended in ACI [7] for RC members in contact with soil under service conditions. The amount of transverse reinforcement in Specimen 4 was determined with Eq. (3), which specifies the minimum required to prevent bar anchorage failure.

Fig. 2 – Test Specimen 1

Table 1 – Specimen characteristics

Parameter	Specimen 1	Specimen 2	Specimen 3	Specimen 4
Column diameter, D_c, mm (ft)	1219 (4)	1219 (4)	1219 (4)	1219 (4)
Pile diameter, D_p, mm (ft)	1829 (6)	1829 (6)	1829 (6)	1524 (5)
Column aspect ratio	4.0	4.5	4.5	4.0
Column long. steel (reinforcement ratio)	18 No. 11 (1.55%)	18 No. 14 (2.24%)	18 No. 14 (2.24%)	32 No. 8 (1.40%)
Pile long. steel (reinforcement ratio)	28 No. 14 (1.55%)	26 No. 18 (2.55%)	26 No. 18 (2.55%)	40 No. 11 (2.21%)
Trans. steel in plastic-hinge region of column (volumetric ratio)	2 No. 5 at 165 mm (6.5 in.) (0.87%)	2 No. 5 at 102 mm (4 in.) (1.41%)	2 No. 5 at 102 mm (4 in.) (1.41%)	No. 6 at 102 mm (4 in.) (1.0%)
Formula for embedment length of column reinforcement in pile shaft	$D_{c,\max} + l_d$	$l_d + s + c$	$l_d + s + c$	$l_d + s + c$
Formula for transverse steel in bar anchorage region of pile shaft	Compression Member – AASHTO (2010)	Eq. (2)	Eq. (4)	Eq. (3)

Note: No. 5 = 16 mm, No. 6 = 19 mm, No. 7 = 22 mm, No. 8 = 25 mm, No. 11 = 36 mm, No. 14 = 43 mm, No. 18 = 57 mm.

The concrete for the column and the piles had specified compressive strengths of 31 MPa (4,500 psi) at 28 days. The assemblies were tested when the concrete strengths in the column and the pile were close to 34.5 MPa

(5,000 psi). The reinforcing steel was Grade 60 complying with the ASTM A706 standards [8], and the pile casing was made of A36 steel.

The test specimens were loaded under a constant vertical load that subjected the base of the column to an axial stress equal to 9.4% of the target compressive strength of the concrete, which was 34.5 MPa (5,000 psi). The top of the column was subjected to cyclic lateral displacements in the north-south direction using two 979-kN (220-kip) capacity, 1219-mm (48-in.) stroke, servo-controlled, hydraulic actuators.

2.2 Test results

All four column-pile assemblies had a ductile behavior with plastic hinges forming at the base of the columns. Figure 3 through 6 present the force-drift diagrams and main damages observed in the column-pile connections of Specimens 1 through 4, respectively. The tests were stopped at high ductility demands when the lateral load capacity started to drop significantly due to the buckling and the subsequent low-cycle fatigue fracture of one or more longitudinal bars at the base of the column. Damage in the piles was mainly limited to splitting cracks induced by bar slip and the prying action of the columns, and local cone-shaped fractures near the base of the column. The degree of damage in the piles varied among the specimens. Specimen 2 showed more severe damage in the pile than that of Specimen 1 due to the larger splitting forces generated by the larger diameter bars and the more severe bar slip induced by the shorter embedment length and higher ductility of the column. Splitting cracking in the pile of Specimen 4 was slightly more severe than that of Specimen 2 due to the smaller pile diameter which resulted in a thinner concrete ring to resist the splitting forces induced by slip. The pile of Specimen 3 had very minor damage owing to the effectiveness of the steel casing in restraining the opening of the splitting cracks.

The contributions of the flexural deformation, base rotation, and shear deformation of the columns to the total lateral displacements of the columns of Specimens 1 and Specimens 2 at different levels of displacement ductility are shown in Table 2. The displacement ductility μ is defined as the ratio of the lateral displacement of the specimen to the effective yield displacement as defined in [5]. The contributions of different mechanisms to the lateral displacement of a column have been calculated by Liu [9] based on measurements of displacement transducers installed in the specimens and strain gages along the embedment length of the column longitudinal reinforcement. As shown in Table 2, the base rotation caused by strain penetration and bar slip had a significant contribution to the lateral displacement of a column (between 30% and 45%). Column flexure had the most significant contribution (between 55% and 70%) while the contribution of the shear was negligible (less than 4%). For the last cycles of the tests, the contributions from flexural deformation and base rotation are lumped because the rotational displacement due to the strain penetration cannot be obtained due to the damage in the strain gauges on the bars at the column-pile interface.

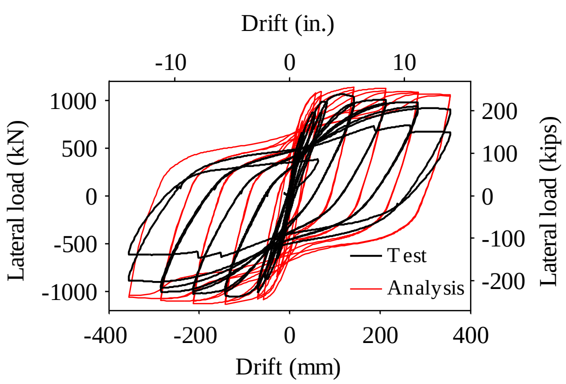

(a) Lateral force-drift diagram

(b) Damage in the column-pile connection

Fig. 3 – Response of Specimen 1

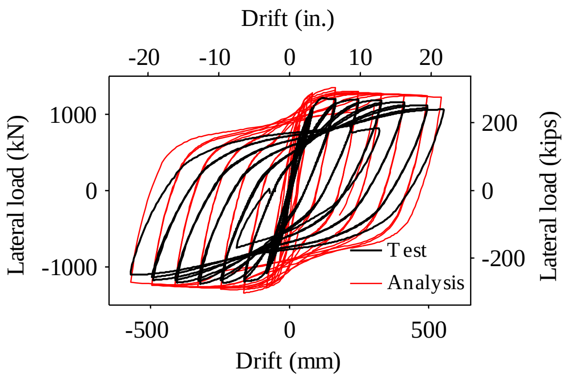

(a) Lateral force-drift diagram

(b) Damage in the column-pile connection

Fig. 4 – Response of Specimen 2

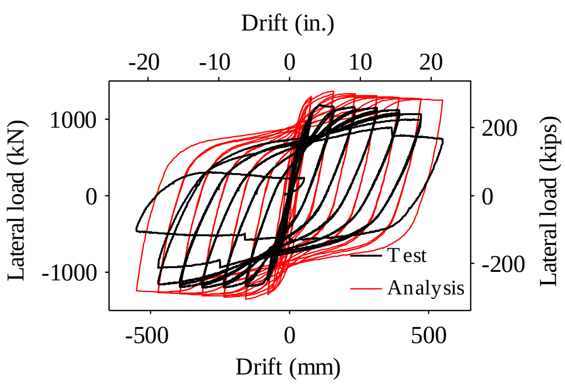

(a) Lateral force-drift diagram

(b) Damage in the column-pile connection

Fig. 5 – Response of Specimen 3

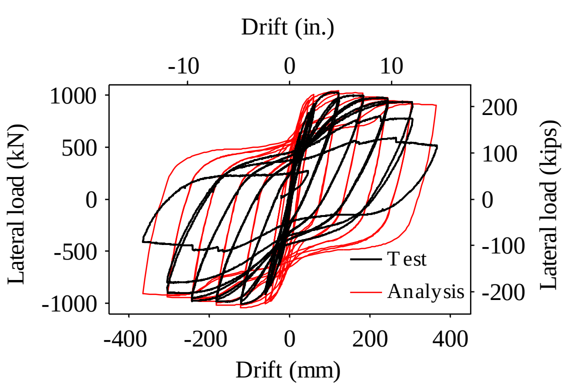

(a) Lateral force-drift diagram

(b) Damage in the column-pile connection

Fig. 6 – Response of Specimen 4

Table 2 – Sources of column deformation

Specimen	Ductility demand, μ	% Flexural deformation	% Base rotation	% Shear deformation
Specimen 1	1.1	56.1%	43.1%	0.8%
	3.3	65.3%	32.9%	1.8%
	5.5	96.4%		3.6%
Specimen 2	1.0	67.2%	32.2%	0.6%
	3.0	67.1%	30.9%	2.0%
	5.0	98.8%		1,2%
	6.9	98.3%		1.7%

Figure 7 shows the strains in the column longitudinal bar at the north extreme face of Specimens 2 and 3. As shown, plastic strains developed near the base of the columns and penetrated into the bar anchorage region of the piles. The extent of plastic strain penetration depends on the bond between the bar and the surrounding concrete. A weaker bond will result in more severe plastic strain penetration, which will in turn reduce the bond strength between the bar and the surrounding concrete, as shown in Shima et al. [10]. For Specimen 2, the maximum plastic strain penetration measured in the bars at $\mu = 5.5$ was 50% of the embedment length. The strain gages were damaged at higher ductility demands. For Specimen 3, most of the strain gages provided reliable readings until the end of the test, and the maximum plastic strain penetration measured at $\mu = 6.3$ was 33% of the embedment length. This reduction in the plastic penetration can be attributed to the higher amount of confinement provided by the steel casing, which improved the bond resistance between the bars and the surrounding concrete, as compared to Specimen 2.

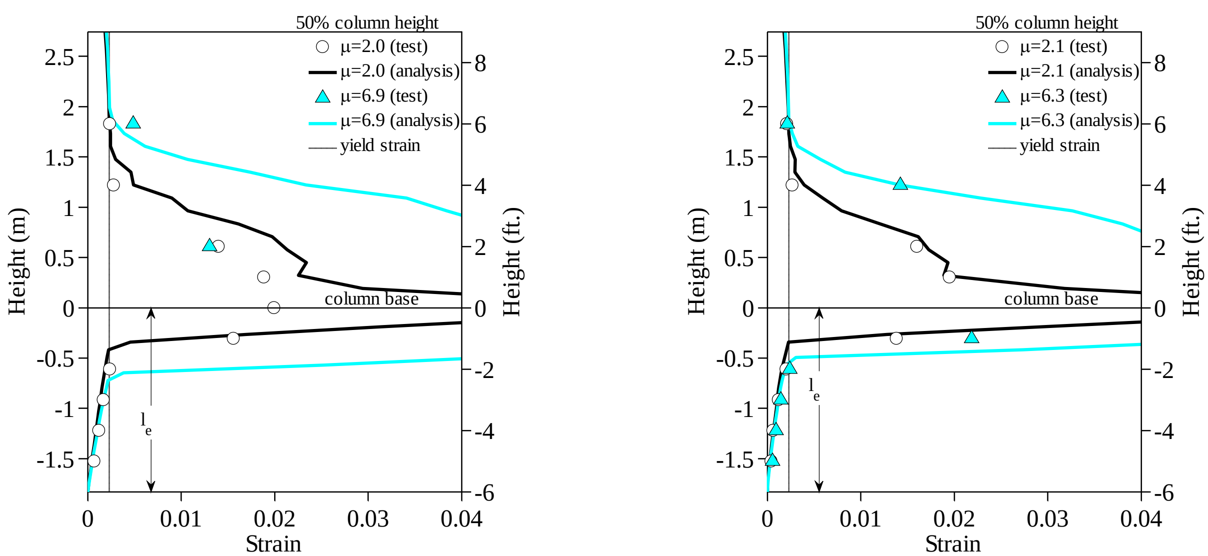

(a) Specimen 2 (b) Specimen 3

Fig. 7 – Strain distribution along column longitudinal bars

4. Finite element modeling of column-pile assemblies

Nonlinear finite element models of the column-pile tests have been developed using Abaqus [11]. Fig. 8 shows the model for one of the specimens. Only half of the specimen is modeled by taking advantage of the symmetry plane in the loading (north-south) direction. Concrete is modeled with solid elements and a damage-plastic model available in Abaqus. Steel is modeled with an elasto-plastic model with linear kinematic hardening. Longitudinal reinforcing bars are modeled with beam elements. The bond-slip behavior of these bars is simulated with an interface element that connects the concrete and the steel elements, as shown in Fig. 8. This element has been developed and implemented in Abaqus with a user subroutine by Murcia-Delso and Shing [12]. Perfect bond is assumed for the transverse reinforcement, which is modeled with truss elements embedded in the concrete elements. The steel casing of Specimen 3 is modeled with shell elements.

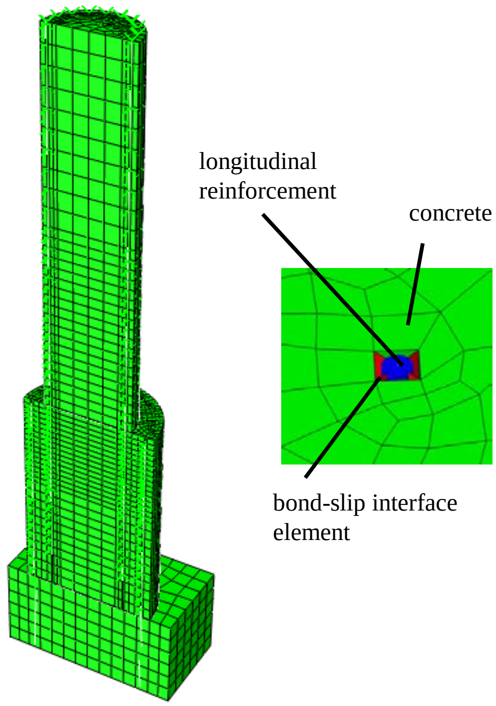

Fig. 8 – Finite element model of a test specimen

The lateral load-vs.-drift relations obtained from the analyses are compared to the test results in Fig. 3 through 6. As shown, the numerical results match the test results well, except for the last few cycles of the tests. The discrepancy for the later cycles is mainly due to the fact that the FE models do not account for the buckling and fracture of the longitudinal bars, which were observed near the base of the columns.

Figure 7 compares the numerical and experimental results on the variation of the tensile strains in the column longitudinal bars located at the north extreme face of the specimens. As shown, the strain variations along the embedment length of the bars are reasonably well predicted by the models, indicating that the bond-slip behavior of the bars is well represented. For Specimen 3, the maximum plastic strain penetration obtained with the FE models match the test results well. For Specimen 2, strain gages were damaged in the last few cycles, and the maximum plastic strain penetration could not be obtained.

The bond stresses along the embedment length of the column bars obtained from FE analysis are plotted in Fig. 9. The stresses plotted are at the peak displacements of different cycles when the bars are in tension. For Specimen 1, which had an embedment length of $D_c + l_d$, the bond stresses along the anchorage length are highly non-uniform. The peak bond stress occurs near the top of the embedment length at the beginning, and its location moves downward as the displacement demand increases due to progressive bond deterioration caused by increased slip and tensile yielding of the bar at the top. In the lower half of of the embedment length, little bond resistance is activated. This indicates that a significant portion of the embedment length is not utilized to develop the bar stress. Specimens 2 and 4, which have a reduced embedment lengths of $l_d + s + c$, show a different bond-stress distribution pattern. The upper potion of the embedment length has deteriorated significantly when the displacements are equal to the maximum reached in the tests, and along the remaining bar embedment lengths, the bond stresses are more or less uniform. These results indicate that the bars have experienced more slip and the bond capacities are more fully utilized along the embedment regions, with little extra anchorage capacity. Figure 9 also shows that the use of the steel casing around the pile in Specimen 3 has resulted in bond-stress distributions similar to those for Specimen 1, even though it has the same embedment length as Specimen 2. These results indicate the benefit of added confinement due to the steel casing.

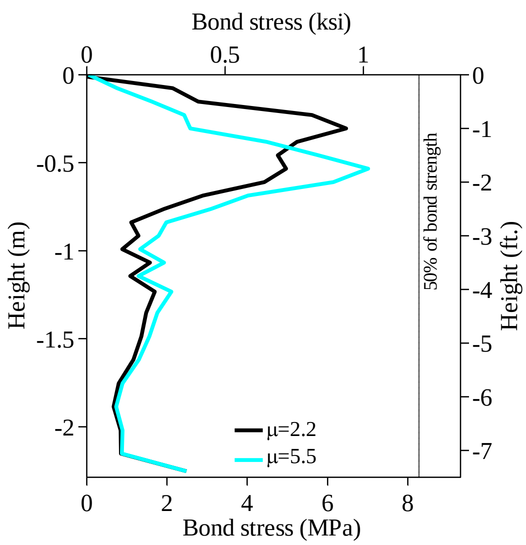

(a) Specimen 1

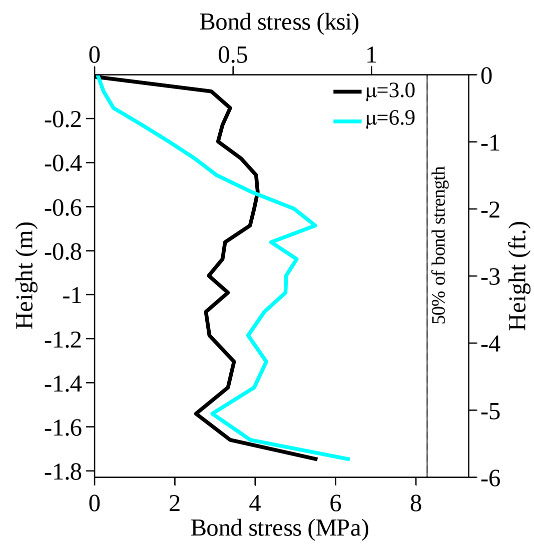

(b) Specimen 2

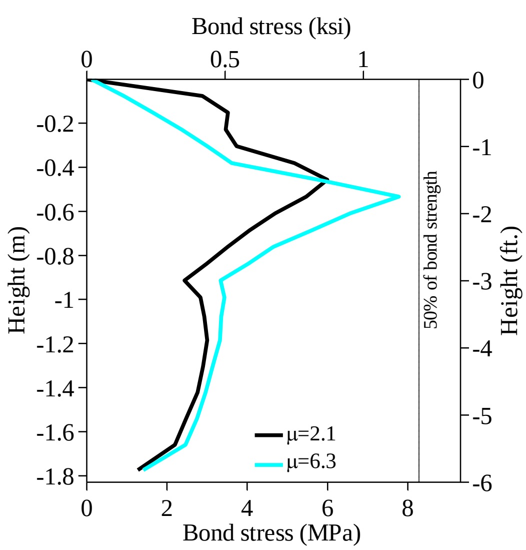

(c) Specimen 3

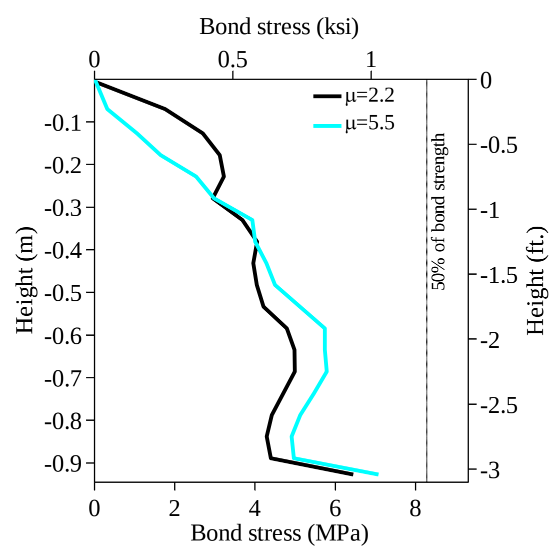

(d) Specimen 4

Fig. 9 – Bond-stress distribution along column longitudinal bars

5. Conclusions

Results of this investigation have shown that an embedment length of $l_d + s + c$ is sufficient to develop the tensile strength of longitudinal reinforcement in bridge columns extended into oversized pile shafts. Adequate transverse reinforcement must be provided in the bar anchorage region of a pile shaft to control tensile splitting cracks induced by bar slip and the prying action of the column. The tests and finite element analyses have shown that an engineered steel casing can effectively arrest tensile splitting cracks in a pile shaft and improve bond performance along the embedment length of the column reinforcement in the pile shaft.

6. Acknowledgements

Funding for the research presented in this paper was provided by Caltrans under Contract No. 59A0710. The authors would like to acknowledge the constructive input of Mark Mahan and Charles Sikorsky to this study, and the technical staff of the Powell Structural Engineering Laboratories for their assistance in the experimental work. However, the opinions expressed in this paper are those of the authors and do not necessarily reflect those of the sponsor.

7. References

[1] California Department of Transportation (Caltrans) (2013): *Caltrans Seismic Design Criteria, Version 1.7*, Sacramento, CA.

[2] American Association of State Highway and Transportation Officials (AASHTO) (2011): *AASHTO LRFD Seismic Bridge Design Specifications*, 2nd Edition, Washington DC, USA.

[3] McLean, D.I., Smith, C.L. (1997): Noncontact lap splice in bridge column-shaft connections. *Report No. WA-RD 417.1*, Washington State Transportation Center, Washington State University, Pullman, USA.

[4] American Association of State Highway and Transportation Officials (AASHTO) (2010): *LRFD Bridge Design Specifications*, 5th Edition, Washington DC, USA.

[5] Murcia-Delso, J., Shing. P.B., Stavridis, A., Liu, Y. (2013): Required Embedment Length of Column Reinforcement Extended into Type II Shafts. *Report No. SSRP–13/05*, Structural Systems Research Project, Department of Structural Engineering, University of California, San Diego, USA.

[6] Murcia-Delso, J., Stavridis, A., Shing, P.B. (2013): Bond strength and cyclic bond deterioration of large-diameter bars. *ACI Structural Journal*, **110** (4), 659-670.

[7] American Concrete Institute (ACI) (2001): Control of Cracking of Concrete Structure. *ACI 224R-01*, Farmington Hills, USA,

[8] ASTM International (2009): *A706/A706M-09b Standard Specification for Low-Alloy Steel Deformed and Plain Bars for Concrete Reinforcement*, West Conshohocken, USA.

[9] Liu, Y. (2012): *Lateral Behavior of Reinforced Concrete Columns Supported on Type II Shafts*. MS Thesis, Department of Structural Engineering, University of California, San Diego, USA.

[10] Shima, H., Chou, L., Okamura, H. (1987): Bond Characteristics in Post-Yield Range of Deformed Bars. *Proceedings of JSCE*, **378** (6), 113-124.

[11] Simulia (2010): *Abaqus V. 6.10*, Dassault Systemes Simulia Corp., Providence, USA,

[12] Murcia-Delso, J., Shing. P.B., (2014): Bond-Slip Model for Detailed Finite Element Analysis of Reinforced Concrete Structures. *Journal of Structural Engineering*, 10.1061/(ASCE)ST.1943-541X.0001070, 04014125.